Calculating state-to-state transition probabilities within time-dependent density-functional theory

Nina Rohringer,* Simone Peter, and Joachim Burgdörfer
Institute for Theoretical Physics, Vienna University of Technology, A-1040 Vienna, Austria
(Received 8 August 2005; published 24 October 2006)

The determination of the elements of the S matrix within the framework of time-dependent density-functional theory (TDDFT) has remained a widely open question. We explore two different methods to calculate state-to-state transition probabilities. The first method closely follows the extraction of the S matrix from the time-dependent Hartree-Fock approximation. This method suffers from cross-channel correlations resulting in oscillating transition probabilities in the asymptotic channels. An alternative method is proposed, which corresponds to an implicit functional of the time-dependent density. Evaluated with the exact time-dependent density it gives rise to stable and accurate transition probabilities. However, the functional shows an extreme sensitivity with respect to errors in the time-dependent density when evaluated using an approximate density from an actual TDDFT calculation. Two exactly solvable two-electron systems serve as a benchmark for a quantitative test.

DOI: 10.1103/PhysRevA.74.042512 PACS number(s): 31.15.Ew, 31.10.+z, 32.80.Wr, 34.50.Pi

I. INTRODUCTION

As a matter of principle, time-dependent density-functional theory (TDDFT) [1] provides a highly efficient method to solve the time-dependent quantum many-body problem. It yields directly the time-dependent one-particle density $n(\vec{r},t)$ of the many-body system. All physical observables of the quantum system can, in principle, be determined from the density. In practice there are two essential ingredients to a TDDFT calculation. First, an approximation to the time-dependent exchange-correlation potential $V_{xc}[n](\vec{r},t)$ has to be found, which via the noninteracting Kohn-Sham system determines the evolution of the density. The second ingredient are functionals that allow the extraction of physical observables from the density. For some of the observables, such as the ground-state energy, extraction is straightforward within ground-state density-functional theory [2]. The time-dependent dipole moment, which governs the emission of high-harmonic radiation can be directly determined from $n(\vec{r},t)$. Excited-state spectra have been obtained from linear-response functionals [3,4]. Other read-out functionals are only approximately, if at all, known. For example, ionization probabilities have been approximately extracted by identifying the integrated density beyond a certain critical distance from the bound system with the flux of ionized particles [5,6]. However, in general, on the most fundamental level, state-to-state transition probabilities contain the full and most detailed information on the response of a many-body system to an external perturbation within the Schrödinger theory. One example is bound-bound transition amplitudes required, e.g., in coherent control calculations of laser-matter interactions within the TDDFT [7], currently a hot topic since attosecond laser pulses influence the electron dynamics.

The ultimate goal of the study of the (in general) nonlinear response of the many-body system to a time-dependent perturbation within Schrödinger theory is the determination of the state-to-state transition amplitude

$$S_{i,f} = \lim_{t\to\infty} \langle \chi_f | U(t,-t) | \chi_i \rangle, \tag{1}$$

where $|\chi_{i,f}\rangle$ are the initial (final) channel states of the system prior to (i) and after (f) the perturbation, and $U(t_1,t_2)$ is the time-evolution operator of the system. This poses the fundamental question: How can equivalent information be obtained by the TDDFT? Specifically, can we construct a functional $S_{i,f}[n]$ that allows us to extract $S_{i,f}$ from the TDDFT?

The present paper addresses methods to extract transition probabilities between discrete states of the many-body system. As a point of reference, we investigate first the evaluation of Eq. (1) employing Kohn-Sham orbitals in close analogy to the time-dependent Hartree-Fock (TDHF) method (see Refs. [8–11] and references therein). This method would be the equivalent of the time-dependent many-body perturbation theory in which the time-dependent noninteracting Kohn-Sham system is considered as the unperturbed system. This method involves three steps of approximations: the initial state, the final state, and the many-body propagator are approximated by their TDDFT equivalents. We encounter similar conceptual problems ("cross-channel correlations") as the TDHF does. We then formulate a functional that, in principle, allows the determination of $S_{i,f}[n]$, which is shown to be free of these deficiencies. We test the method with the help of two exactly solvable one-dimensional two-electron systems, a harmonic oscillator, and a helium model. We show that its accuracy is limited by the extreme sensitivity to the error in the density $n(\vec{r},t)$.

The article is organized as follows. In Sec. II we introduce the approximation to calculate the S matrix within the TDDFT based on the time-dependent Kohn-Sham orbitals. Furthermore, the new read-out functional is derived, which allows us to calculate state-to-state transition probabilities directly from the time-dependent density. In Sec. III we present numerical tests on two different one-dimensional

*Present address: Argonne National Laboratory, Argonne, IL 60439, USA. Electronic address: nrohringer@anl.gov

model systems. Orbital-based approaches to calculate the S matrix are compared to the density-based approach. Atomic units ($|e|=\hbar=m=1$) are used throughout.

II. READ-OUT FUNCTIONALS FOR TRANSITION PROBABILITIES

We consider an interacting N-electron system of Hamiltonian H_0 with stationary eigenstates $\chi_{i,f}$, which is subject to a perturbation $V(t)$ which is switched on at time $t=0$ and switched off at time $t=\tau$. The initial state of the system $|\chi_i\rangle$ is assumed to be the ground state and evolves according to the time-dependent many-body Schrödinger equation

$$i\frac{\partial}{\partial t}|\Psi(t)\rangle = [H_0 + V(t)]|\Psi(t)\rangle, \quad |\Psi(0)\rangle = |\chi_i\rangle. \tag{2}$$

The state-to-state transition amplitude (or S matrix) from the initial state $|\chi_i\rangle$ to a final state $|\chi_f\rangle$ is defined by the overlap of the propagated state $|\Psi(t)\rangle$ with eigenstates $|\chi_f\rangle$ of the unperturbed system

$$S_{i,f} = \lim_{t\to\infty}\langle\chi_f|\Psi(t)\rangle. \tag{3}$$

For later reference we note that the time evolution of the transition amplitude for $t>\tau$ is given in terms of the eigenenergies of the asymptotic final states ε_f by

$$\langle\chi_f|\Psi(t)\rangle = \exp[-i\varepsilon_f(t-\tau)]\langle\chi_f|\Psi(\tau)\rangle. \tag{4}$$

Since the perturbation vanishes for $t>\tau$, the state-to-state transition probability is given by $P_{i,f}=|S_{i,f}|^2=|\langle\chi_f|\Psi(\tau)\rangle|^2 = \lim_{t\to\infty}|\langle\chi_f|\Psi(t)\rangle|^2$.

Within the TDDFT, the time-dependent density is represented through the time-dependent Kohn-Sham spin orbitals $\Phi_{\sigma,j}(\vec{r},t)$ as

$$n(\vec{r},t) = \sum_{\sigma=\uparrow,\downarrow} n_\sigma(\vec{r},t) = \sum_{\sigma=\uparrow,\downarrow}\sum_{j=1}^{N_\sigma}|\Phi_{\sigma,j}(\vec{r},t)|^2, \tag{5}$$

where N_σ denotes the number of electrons of spin σ. The one-particle spin orbitals $\Phi_{\sigma,j}(\vec{r},t)$ evolve according to the time-dependent Kohn-Sham equations governed by the Hamiltonian

$$H_\sigma^{KS}[n_\uparrow,n_\downarrow] = -\frac{1}{2}\vec{\nabla}^2 + V_{ext}(\vec{r}) + V(\vec{r},t) + V_H[n](\vec{r},t) + V_{xc}[n_\uparrow,n_\downarrow](\vec{r},t), \tag{6}$$

which includes the external time-independent and time-dependent one-particle potentials $V_{ext}(\vec{r})$ and $V(\vec{r},t)$, the Hartree potential $V_H[n](\vec{r},t)$, and the exchange-correlation potential $V_{xc}[n_\uparrow,n_\downarrow](\vec{r},t)$. The initial states $|\Phi_{\sigma,j}(0)\rangle=|\Phi_{\sigma,j}\rangle$ are the occupied Kohn-Sham orbitals of stationary ground-state density-functional theory (DFT). Although Kohn-Sham orbitals have, *a priori*, no physical meaning as single-particle quantum states, the Slater determinant of Kohn-Sham orbitals,

$$|\Psi^{\mathrm{TDDFT}}\rangle := \hat{A}|\Phi_{\uparrow,1},\ldots,\Phi_{\uparrow,N_\uparrow},\Phi_{\downarrow,1},\ldots,\Phi_{\downarrow,N_\downarrow}\rangle, \tag{7}$$

where $\hat{A}$ denotes the operator for antisymmetrization, may be interpreted as a zeroth-order approximation to the many-body wave function in terms of coupling-constant perturbation theory [12,13]. It is therefore tempting to determine, in analogy to the TDHF approximation [8–11], an approximate S matrix as the transition amplitude

$$S_{i,f}(t) \simeq \langle\chi_f|\Psi^{\mathrm{TDDFT}}(t)\rangle. \tag{8}$$

A delicate question arises at this point: Which are the appropriate channel states $\chi_{i,f}$ to project on? For the initial state, stationarity of the propagation of the system in the limit of a vanishing external perturbation $[V(\vec{r},t)=0]$ mandates that χ_i is a Kohn-Sham Slater determinant of the occupied ground-state orbitals. No such restriction is imposed on χ_f when the evolution is calculated by forward propagation. The simplest choice for channel states $|\chi_f\rangle$ are Kohn-Sham Slater determinants built up from occupied and virtual Kohn-Sham orbitals $|\Phi_{\sigma,j}\rangle$ of the ground-state DFT problem, i.e.,

$$S_{i,f} \cong \lim_{t\to\infty}\langle\chi_f^{\mathrm{DFT}}|\Psi^{\mathrm{TDDFT}}(t)\rangle. \tag{9}$$

Reliable transition probabilities can only be expected if both, time-dependent and stationary Kohn-Sham Slater determinants are good approximations to the time-dependent and stationary many-body wave functions, respectively. Therefore, different choices of $|\chi_f\rangle$ need to be explored. For example, excited states often show a higher degree of correlation than ground states and a single Kohn-Sham Slater determinant is obviously no longer a satisfactory approximation. In such cases, more elaborate final-state channel functions are needed. Alternatively, configuration-interaction (CI) or multiconfiguration Hartree-Fock (MCHF) can be employed [14,15]. Within the TDDFT, linear-response theory allows the calculation of the excitation spectrum by including particle-hole excitations [3,4]. As a byproduct, improved excited states, i.e., the particle-hole reduced-density matrix, are generated in terms of an expansion in single-particle excitations of Kohn-Sham orbitals. The applications we are studying in Sec. III are restricted to two-electron systems. In this case the linear-response approach should give an improved wave function compared to the initial single Kohn-Sham Slater determinant [16]. As discussed below, this and other approaches to $|\chi_f\rangle$ suffer from similar shortcomings, as does Eq. (9).

We therefore introduce a new functional which depends only on the time-dependent density $n(\vec{r},t)$, thus adhering to the spirit of the TDDFT. For simplicity and in line with the model systems studied in Sec. III, the derivation is presented for two-electron systems. Generalizations to arbitrary many-electron systems are straightforward.

The starting point is the expansion of the exact time-dependent wave function in terms of a complete set of final-state wave functions

$$\Psi(\vec{r}_1,\vec{r}_2,t) = \sum_f \langle\chi_f|\Psi(t)\rangle\chi_f(\vec{r}_1,\vec{r}_2). \tag{10}$$

Using the stationary one-particle reduced-density matrix

$$\rho^{(1)}_{f'f}(\vec{r}) = 2\int d\vec{r}_2 \chi^*_{f'}(\vec{r},\vec{r}_2)\chi_f(\vec{r},\vec{r}_2) \tag{11}$$

and the time-dependent transition-density matrix defined by

$$T_{f,f'}(t) = \langle \chi_f|\Psi(t)\rangle\langle\Psi(t)|\chi_{f'}\rangle, \tag{12}$$

the exact time-dependent density is given by

$$n(\vec{r},t) = \sum_{f,f'} T_{f,f'}(t)\rho^{(1)}_{f'f}(\vec{r}) = \mathrm{Tr}[T(t)\rho^{(1)}(\vec{r})]. \tag{13}$$

The transition-density matrix can be directly determined by the inversion of Eq. (13). Our primary interest lies in the transition probabilities $|S_{i,f}|^2$, i.e., the diagonal elements ($f'=f$) of the transition-density matrix $T_{f,f'}(t)\to S_{i,f}(t)S^*_{i,f'}(t)$ at times after the switch off of the external perturbation $t>\tau$. In this case the inversion problem of dimension $N_f\times N_f$ (N_f: dimension of truncated final-state space considered) can be drastically simplified. Using Eq. (4), for nondegenerate final states ($\varepsilon_f\neq\varepsilon_{f'}$), the transition probabilities T_{ff} can be extracted from a time average over an interval $(t-\tau)|\varepsilon_{f'}-\varepsilon_f|\gg 2\pi$,

$$\bar{n}(\vec{r},t) := \int_\tau^t \frac{n(\vec{r},t')}{t-\tau}dt' = \sum_{f,f'}\rho^{(1)}_{f'f}(\vec{r})\int_\tau^t \frac{T_{f,f'}(t')}{t-\tau}dt', \tag{14}$$

leading to the implicit read-out functional

$$\lim_{t\to\infty}\bar{n}(\vec{r},t) = \sum_f \rho^{(1)}_{f,f}(\vec{r})|S_{i,f}|^2. \tag{15}$$

Unlike Eq. (13), Eq. (15) requires only an N_f-dimensional inversion. In practice, the application of Eq. (15) requires evaluating the final-state densities $\rho^{(1)}_{f,f}(\vec{r})$ at N_f distinct points $\vec{r}_j$, $j=1,\ldots,N_f$, so that the matrix $R_{j,f}:=\rho^{(1)}_{f,f}(\vec{r}_j)$ does not become near singular and remains invertible. The state-to-state transition probabilities then become

$$|S_{i,f}|^2 = \lim_{t\to\infty}\sum_{j=1}^{N_f}\bar{n}(\vec{r}_j,t)R^{-1}_{j,f}, \quad f=1,\ldots,N_f. \tag{16}$$

The necessary information to calculate state-to-state transition amplitudes are therefore the time-dependent density $n(\vec{r},t)$ and the stationary densities of the final states $\rho^{(1)}_{f,f}(\vec{r})$ (densities of the excited eigenstates of the many-electron system). The densities $\rho^{(1)}_{f,f}(\vec{r})$ (except for the ground-state density) are not readily accessible within the TDDFT or ground-state DFT. TDDFT linear-response theory in principle provides exact excitation energies of the many-electron system and may also provide a recipe to determine excited-state densities [28]. Since the TDDFT, in principle, determines the exact time-dependent density, uncertainties in $\rho^{(1)}_{f,f}(\vec{r})$ represent therefore one major limitation to the applicability and accuracy of Eq. (16), not directly related to the TDDFT itself.

III. NUMERICAL TESTS

We have tested the two functionals of Eqs. (9) and (16) for two exactly solvable one-dimensional two-electron systems.

A. Harmonic two-electron quantum dot

The first system consists of two electrons confined to a harmonic quantum dot [17,18]. In its present one-dimensional (1D) version, the electron-electron interaction must be replaced by a screened Coulomb potential [19] to allow the electrons to bypass each other. The Hamiltonian of the system is given by

$$\hat{H}_{dot}(t) = \sum_{i=1,2}\left(\frac{\hat{p}_i^2}{2}+\frac{\omega^2}{2}x_i^2 - F(t)x_i\right) + \frac{1}{\sqrt{b+(x_1-x_2)^2}}, \tag{17}$$

where x_i and p_i are the coordinates and momenta of electron i ($i=1,2$). The softening parameter b is set to $b=0.55$. The laser field

$$F(t) = F_0\sin(\omega_L t)\times\begin{cases} 3t/\tau & t\le\tau/3,\\ 1 & \tau/3<t<2\tau/3,\\ 3(\tau-t)/\tau & 2\tau/3<t<\tau,\\ 0 & t\ge\tau,\end{cases} \tag{18}$$

with driving frequency $\omega_L=0.1839$ is treated in dipole approximation. The pulse length is chosen as $\tau=168$ and the field amplitude is $F_0=0.07$. Introducing center-of-mass (c.m.) coordinates $R=x_1+x_2$ and relative coordinates $r=x_1-x_2$, the Schrödinger equation (2) can be separated, since the Hamiltonian of Eq. (17) splits into $\hat{H}=\hat{H}_{rel}+\hat{H}_{\mathrm{c.m.}}(t)$. The eigenstates of the unperturbed system are characterized by the set of quantum numbers $(N_{\mathrm{c.m.}},n_{rel})$, the number of nodes of the c.m. and relative wave function. The initial state is the spin-singlet ground state $|N_{\mathrm{c.m.}}=0,n_{rel}=0\rangle$. The time dependence of the total Hamiltonian is confined to the c.m. Hamiltonian. The exact time-dependent wave function therefore separates into a time-dependent c.m. and a time-independent relative part, $\Psi(r,R,t)=g(r)h(R,t)$. Since the system starts out from the ground state, $h(R,t)$ represents a coherent state of the 1D harmonic oscillator driven by an external electric field. The dynamics of the density of this model system is subject to the harmonic potential theorem [20,21], i.e., the density is rigidly shifted without any distortion. For the present system, exact excited final states can be easily calculated.

In the case of a two-electron spin-singlet system evolving from the ground state, the time-dependent Kohn-Sham scheme consists in solving the Kohn-Sham equation for one doubly occupied Kohn-Sham orbital $\Phi(x,t)$. For spin-unpolarized two-particle systems the exact $V_{xc}(t)$ can be constructed using the exact density derived from the Schrödinger equation and inverting the Kohn-Sham equation [22,23,29,30]. Since the harmonic two-electron quantum dot satisfies the harmonic potential theorem, the time dependence of the exchange-correlation potential is a rigid shift and the exact $V_{xc}(t)$ is easily constructed. We also employed the adiabatic local spin-density approximation (ALSDA) with the self-interaction correction (SIC) [24]. Since no reliable correlation potential is available for a 1D electron system we only consider exchange. The L_1 norm $\delta n(t)$ of the

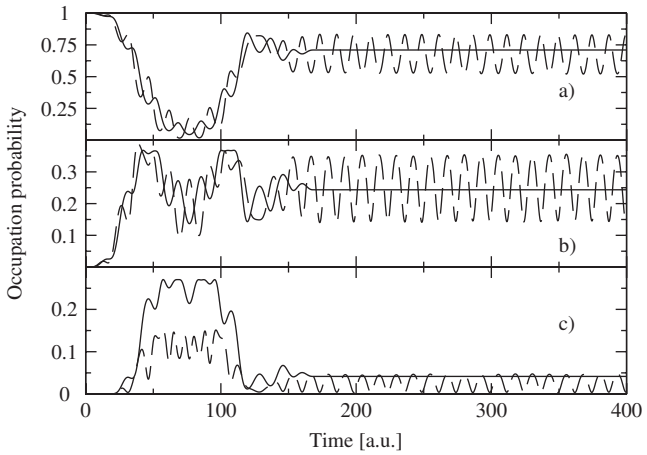

FIG. 1. Ground- and excited-state transition probabilities for the laser-driven harmonic 1D two-electron quantum dot of a confining frequency $\omega=0.25$ in the dependence of time: Comparison of occupation probabilities of the ground state (a), first excited state $|N_{\text{c.m.}}=1,n_{rel}=0\rangle$ (b), and second excited state $|N_{\text{c.m.}}=2,n_{rel}=0\rangle$ (c) of the exact calculation (full line) and the TDDFT calculation (dashed line). The TDDFT occupation probabilities are obtained using the approximate S matrix Eq. (9); final channel states are Slater determinants of Kohn-Sham orbitals $|0,0\rangle$, $|0,1\rangle$, and $|0,2\rangle$. Parameters of the laser pulse: $F_0=0.07$, $\omega_L=0.1839$, $\tau=168$.

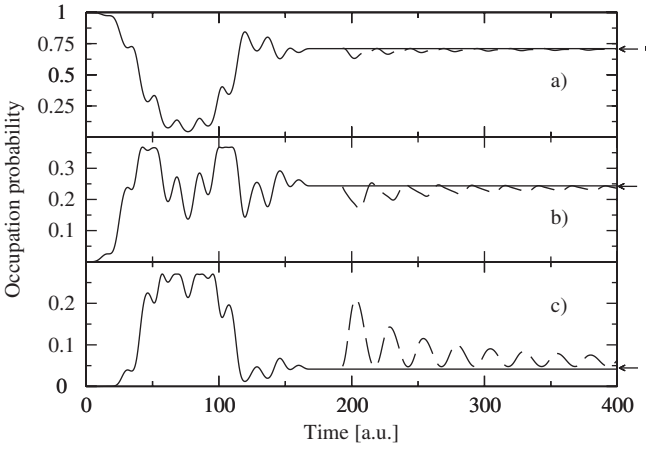

FIG. 2. Ground- and excited-state transition probabilities for the laser-driven harmonic 1D two-electron quantum dot for a confining frequency $\omega=0.25$ in the dependence of time: Comparison of occupation probabilities of the ground state (a), first excited state $|N_{\text{c.m.}}=1,n_{rel}=0\rangle$ (b), and second excited state $|N_{\text{c.m.}}=2,n_{rel}=0\rangle$ (c) of exact calculation (full line) and the TDDFT calculation (dashed line). The TDDFT transition probabilities are obtained by the inversion of Eq. (16). Parameters of the laser pulse: $F_0=0.07$, $\omega_L=0.1839$, $\tau=168$.

deviation between the exact and TDDFT density

$$\delta n(t) = \int |n_{\text{exact}}(x,t) - n_{\text{TDDFT}}(x,t)|dx \tag{19}$$

is about 0.2 for the highly correlated system of $\omega=0.25$. The ground-state Kohn-Sham equation generates a set of excited virtual Kohn-Sham orbitals $|n\rangle$. Figure 1 shows a comparison of exact occupation probabilities and those obtained from the approximate S matrix [Eq. (9)] by projecting $\Psi^{\text{TDDFT}}(t)=\Phi(x_1,t)\Phi(x_2,t)$ onto Kohn-Sham Slater determinants. Shown are the occupation of the ground state [Fig. 1(a), projection onto the Kohn-Sham determinant $|0,0\rangle$], the first excited state [Fig. 1(b), projection onto $|0,1\rangle$], and the second excited state [Fig. 1(c), projection onto $|0,2\rangle$]. The second excited state $|N_{\text{c.m.}}=2,n_{rel}=0\rangle$ involves a configuration mixture of at least two Kohn-Sham Slater determinants to be well represented (configurations $|0,2\rangle$ and $|1,1\rangle$). Neither the projection onto a single Kohn-Sham configuration state $|0,2\rangle$ [Fig. 1(c)] nor the projection onto the exact excited state (not shown) yields satisfactory transition probabilities. After the switchoff of the laser, the density undergoes oscillations resulting in time-dependent Hartree and exchange-correlation potentials, which give rise to oscillations in the occupation probabilities. These are the signatures of the "spurious cross-channel correlations" well known from the TDHF [9,10]. We have checked that cross-channel correlations persist when we project onto exact exit-channel states rather than Kohn-Sham determinants, i.e., replacing $|\chi_f^{\text{DFT}}\rangle$ by $|\chi_f\rangle$ in Eq. (9). Moreover, we have also tested channel states obtained from a TDDFT linear-response (DFT-LR) equation. In this equation the exchange-correlation kernel of the TDDFT was approximated by the exchange-only time-dependent optimized effective potential [4,25] and the exact Kohn-Sham orbitals obtained by the exact ground-state exchange-correlation potential have been used. The obtained excited-state wave functions $|\chi_f^{\text{DFT-LR}}\rangle$, however, do not significantly differ from the single Kohn-Sham Slater determinants although the excitation energies are considerably improved compared to the Kohn-Sham energy differences. With presently available approximations to the exchange-correlation kernel, the TDDFT linear-response theory does not provide substantially improved excited-state wave functions. We thus conclude that the projection approach of Eq. (9) is not well suited to accurately determine the S matrix within the TDDFT, irrespective of the particular choice of $|\chi_f\rangle$.

To test the newly proposed read-out functional, which depends only on the density, we use the exact time-dependent density $n(x,t)$. In this way, errors due to the approximate exchange-correlation potential can be ruled out and the quality of the proposed functional for state-to-state transition probabilities can be directly assessed. Figure 2 shows a comparison of transition probabilities obtained by projecting the wave function according to Eq. (3) (solid line) and by the new density functional of Eq. (16) (dashed line) for the three lowest-lying states. The sum in Eqs. (14)–(16) is truncated after the second excited state. In the limit of $t\to\infty$, i.e., as the averaging interval in Eq. (14) increases, the transition probability converges within the numerical accuracy toward the exact result, marked by arrows. Numerical errors are due to the truncation of the sum over final states in Eq. (16). Note that simply averaging over the cross-channel correlation in Eq. (9) (see Fig. 1) would lead, in general, to incorrect results.

B. 1D helium

As a second test system, which allows also for transitions to the continuum and therefore exhibits more complex dy-

namics, we study a 1D helium model. This model served already in the past to benchmark different approximation regimes [5,15,19,23]. The Hamiltonian of the system is given by

$$\hat{H}_{he} = \sum_{i=1,2} \left[\frac{p_i^2}{2} - \frac{2}{\sqrt{b + x_i^2}} - F(t)x_i \right] + \frac{1}{\sqrt{b + (x_1 - x_2)^2}}. \tag{20}$$

The electric-field amplitude $F(t)$ is given by Eq. (18) with the parameters $\omega_L = 0.0615$, $F_0 = 0.16$, and $\tau = 361$.

In the case of the laser-driven helium an additional challenge is to find an accurate approximation to the exchange-correlation potential, even when the exact density is known. A numerically stable exact exchange-correlation potential has, so far, not been constructed [23]. The cause of the numerical instabilities is similar to those encountered in solving the Schrödinger equation via the hydrodynamic approach to quantum mechanics. The time-dependent doubly occupied orbital is recovered as the ground state of an effective potential (including the exchange-correlation potential). Consequently, this effective potential diverges at the nodes of the density, which makes it numerically difficult to determine the exact exchange-correlation potential by inversion. Exchange-only ALSDA-SIC binds the electrons too strongly and the dynamics of the exact two-electron system is not correctly described. In recent studies, the derivative discontinuity of the time-dependent exchange-correlation potential, with respect to the particle number, was emphasized [23,26] and a new approximate correlation functional mimicking this discontinuity was introduced [23]. The correlation potential in this approximation reads

$$V_c(x,t) = \left[c\left(\frac{N_0(0)}{N_0(t)} \right) - 1 \right] V_H(x,t), \tag{21}$$

where $c(z) = z/(1 + e^{50(z-2)})$ and $V_H(x,t)$ is the Hartree potential. $N_0(t)$ denotes the number of bound states at time t and is approximated by twice the DFT ground-state occupation probability of the time-dependent Kohn-Sham orbital $N_0(t) = 2|\langle \Phi_0 | \Phi(t) \rangle|^2$. At this point it should be mentioned that the exchange-only time-dependent optimized effective potential (TDOEP) [25], within the frame of the KLI approximation [27], also exhibits a derivative discontinuity in the particle number, as was recently pointed out in Ref. [26]. This is, however, only true for systems with at least two electrons of the same spin projection and does not apply to the systems we are studying. In the considered case of a two-electron spin-singlet system the TDOEP-KLI reduces to the exchange-only ALSDA-SIC approach.

In order to assess the quality of the approximate V_c of Eq. (21), independent from the read-out functional, we calculate the time-dependent dipole moment. V_c of Eq. (21) gives slightly better results than the exchange-only ALSDA-SIC. This can be seen in Fig. 3, which compares the time-dependent dipole moment of the exact solution with the dipole moments of the TDDFT calculation based on the ALSDA-SIC and the functional of Eq. (21). The inset of Fig. 3 shows an enlargement of the dipole moment after the turn-

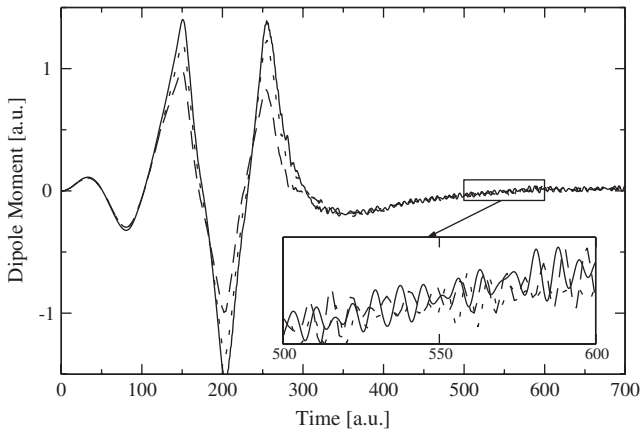

FIG. 3. Comparison of the time-dependent dipole moment of the laser-driven 1D helium of the exact solution (solid line) vs the TDDFT with V_{xc} of Eq. (21) (dotted line) and the ALSDA-SIC exchange only (dashed line). The figure inset is an enlargement of the region after the turnoff of the laser pulse. Parameters of the laser pulse: driving frequency $\omega_L = 0.0615$, field amplitude $A_0 = 0.16$, pulse duration of $\tau = 361$.

off of the laser pulse. In this region the dipole moments of the exact and the different TDDFT solutions show a distinctly different oscillatory behavior, i.e., different frequencies are involved. This demonstrates that the dynamics of the exact density cannot be fully recovered by the approximate TDDFT solutions, even though the differences appear to be small. As will be shown in the following, this causes serious problems for the read-out functional, which directly involves the time-dependent density after the turnoff of the external field.

To show that the read-out functional of Eq. (16) also gives accurate results for the system allowing for a more complex dynamics including ionization, we first evaluate the functional with the exact time-dependent density and the exact final-state densities. Figure 4 compares the result of Eq. (16) with the time-dependent ground-state occupation probability of the exact many-body wave function. Both curves coincide within the numerical accuracy, demonstrating the validity of the read-out functional.

We now turn to the case of an actual TDDFT calculation. In the case of helium, the ground-state occupation of the TDDFT determinant obtained by the projection approach of Eq. (8) evaluated with either the exact many-body ground state or the DFT ground-state determinant gives rise to stable transition probabilities, i.e., the spurious cross-channel correlations are suppressed. Unlike in the case of the harmonic quantum dot, the ground state is the only bound state occupied after the turnoff of the field. The excitation probability is distributed among the continuous spectrum. A considerable amount of flux reached the absorbing boundary. The density hardly undergoes any oscillations or deformations and therefore the exchange-correlation potential is quasistationary. The ionization probability, determined by the loss in norm through the absorbing boundary of the TDDFT system, is slightly lower than in the exact system. The electrons are still too tightly bound in the approximate TDDFT propagation based on V_c of Eq. (21). This is consistent with the

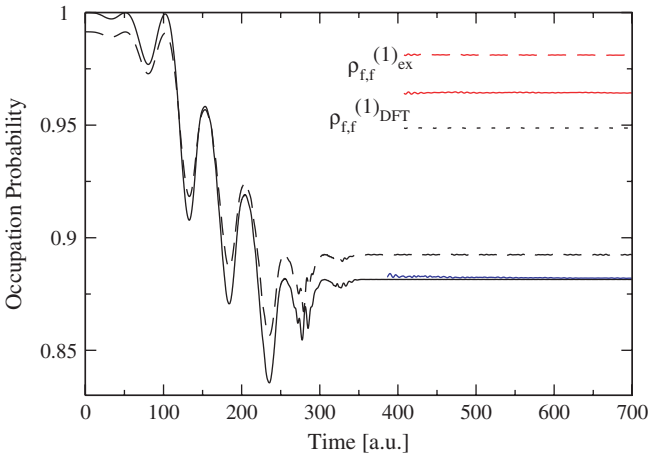

FIG. 4. (Color online) Comparison of ground-state occupation probabilities calculated for the laser-driven 1D He model for several approaches: exact occupation probability calculated by projection of the time-dependent many-body wave function (solid black line starting at $t=0$) compared to the results of Eq. (16) evaluated with the exact time-dependent density and exact final-state densities [solid bold black line starting after the turnoff of the laser pulse, (online: blue)]. The curves are almost indistinguishable within the graphical resolution. The TDDFT ground-state occupation according to the projection approach of Eq. (9) [projection onto the exact many-body ground state (black dashed line)]. The results of the read-out functional of Eq. (16) evaluated for the TDDFT density with the exact final-state densities $\rho_{f,f}^{(1)ex}$ for $N_f=7$ and $N_f=5$ [upper and lower gray solid lines, respectively (online: red lines)]. The results of the read-out functional of Eq. (16) evaluated for the TDDFT density with DFT final-state densities $\rho_{f,f}^{(1)DFT}$ (dotted line).

slightly higher ground-state occupation probability. Because of the absence of discrete cross-channel correlations, the projection approach in this regime gives reasonable but not accurate results.

Applying the read-out functional of Eq. (16) to calculate state-to-state transition probabilities for the TDDFT density we distinguish two different cases, which differ in the final-state densities applied. In the first case we consider the exact final-state density matrix $\rho_{f,f}^{(1)ex}$. Increasing the number of excited states in the truncated space of final states N_f results in a slowly or nonconvergent series of transition probabilities. As can be seen in Fig. 4, the transition probability jumps by increasing N_f and we could not reach converged results for $N_f=7$. By contrast, using the exact time-dependent density, convergence is reached already for $N_f=4$. This is a hint that the problem lies in the incorrect dynamics of the TDDFT density (see the inset in Fig. 3) rather than the convergence properties of the series with respect to N_f. The choice of the exact final-state densities is therefore not well adapted to the approximate TDDFT calculation. We therefore constructed as a second choice DFT final-state densities $\rho_{f,f}^{(1)DFT}$ from single Slater determinants of DFT orbitals. The transition probabilities evaluated by Eq. (16) rapidly converge with respect to N_f. The converged result for the ground-state occupation, however, shows a considerable discrepancy to the exact solution. In fact, the projection approach gives results in better agreement with the exact result.

The important observation is that the read-out functional sensitively depends on the dynamics of the density. Although in the present case the approximated exchange-correlation potential gives overall good results for one-particle expectation values, i.e., the dipole moment, it does not guarantee a reliable determination of transition probabilities. This observation suggests fundamental limitations to the determination of the S matrix, or equivalently n-particle correlation functions from the density $n(\vec{r},t)$ and thus from the TDDFT. The functional $S_{i,f}[n]$ displays an extreme sensitivity to the errors in the density $n(\vec{r},t)$. $n(\vec{r},t)$ involves the information compression from the N-particle density to the one-particle density. Conversely, reconstructing the N-particle density or the full S matrix from the reduced one-particle density involves the reverse process of information "magnification" or expansion. This process will be extremely sensitive to small errors in $n(\vec{r},t)$, as such errors will be magnified in the extraction process. In line with fundamental theorems of the TDDFT [1] the recovery of $S_{i,f}[n]$ is clearly possible, as demonstrated here for exactly solved systems. For practical TDDFT calculations involving inevitably approximate exchange-correlation functionals, however, the extreme sensitivity to even slight errors in $n(\vec{r},t)$ may pose a major stumbling block for extracting scattering information.

IV. CONCLUSIONS

We have investigated two different methods to extract state-to-state transition amplitudes from the TDDFT calculations. In the first method, the correlated many-body wave function is approximated by a Slater determinant of the time-dependent Kohn-Sham orbitals. This approximate wave function is projected onto appropriate final states (exact states or Kohn-Sham configuration states). The resulting state-to-state transition probabilities suffer oscillations after the switchoff of the external perturbation. The second read-out functional to calculate state-to-state transition probabilities directly involves the time-dependent densities and represents thus a well-suited density functional within the framework of the TDDFT. The problem of cross-channel correlations can be avoided and well-defined transition probabilities can be determined in the asymptotic limit $t\to\infty$. This was demonstrated in the case of two model systems, a 1D harmonic dot and a 1D helium atom in an external laser field for the exact time-dependent densities. While read-out functionals for the S matrix can be constructed, they are shown to be extremely sensitive to small errors in the density. Evaluating the read-out functional with the densities of a TDDFT calculation with error-afflicted exchange-correlation potential gives rise to ambiguous results, reflecting the problems of present-day approximations of exchange-correlation potentials.

ACKNOWLEDGMENTS

This work was supported by FWF-SFB 016. We thank Angel Rubio, Hardy Gross, and Kieron Burke for illuminating discussions.

[1] E. Runge and E. K. U. Gross, Phys. Rev. Lett. **52**, 997 (1984).
[2] P. Hohenberg and W. Kohn, Phys. Rev. **136**, B864 (1964).
[3] M. E. Casida, in *Recent Developments and Applications of Modern Density Functional Theory*, edited by J. M. Seminaro (Elsevier, Amsterdam, 1996), p. 391.
[4] M. Petersilka, E. K. U. Gross, and K. Burke, Int. J. Quantum Chem. **80**, 534 (2000).
[5] D. G. Lappas and R. van Leeuwen, J. Phys. B **31**, L249 (1998).
[6] M. Petersilka and E. K. U. Gross, Laser Phys. **9**, 105 (1999).
[7] J. Werschnik and E. K. U. Gross, J. Chem. Phys. **123**, 62206 (2005).
[8] P. Bonche, S. Koonin, and J. W. Negele, Phys. Rev. C **13**, 1226 (1976).
[9] J. J. Griffin, P. C. Lichtner, and M. Dworzecka, Phys. Rev. C **21**, 1351 (1980).
[10] Y. Alhassid and S. E. Koonin, Phys. Rev. C **23**, 1590 (1981).
[11] J. W. Negele, Rev. Mod. Phys. **54**, 913 (1982).
[12] A. Görling and M. Levy, Phys. Rev. B **47**, 13105 (1993).
[13] A. Görling and M. Levy, Phys. Rev. A **50**, 196 (1994).
[14] M. H. Beck, A. Jäckle, G. A. Worth, and H.-D. Meyer, Phys. Rep. **324**, 1 (2000).
[15] J. Zanghellini, M. Kitzler, T. Brabec, and A. Scrinzi, J. Phys. B **37**, 763 (2004).
[16] Angel Rubio (private communication).
[17] M. Taut, Phys. Rev. A **48**, 3561 (1993).
[18] P. M. Laufer and J. B. Krieger, Phys. Rev. A **33**, 1480 (1986).
[19] R. Grobe and J. H. Eberly, Phys. Rev. A **48**, 4664 (1993).
[20] J. F. Dobson, Phys. Rev. Lett. **73**, 2244 (1994).
[21] G. Vignale, Phys. Rev. Lett. **74**, 3233 (1995).
[22] I. D'Amico and G. Vignale, Phys. Rev. B **59**, 7876 (1999).
[23] M. Lein and S. Kümmel, Phys. Rev. Lett. **94**, 143003 (2005).
[24] J. P. Perdew and A. Zunger, Phys. Rev. B **23**, 5048 (1982).
[25] C. A. Ullrich, U. J. Gossmann, and E. K. U. Gross, Phys. Rev. Lett. **74**, 872 (1995).
[26] M. Mundt and S. Kümmel, Phys. Rev. Lett. **95**, 203004 (2005).
[27] J. B. Krieger, Y. Li, and G. J. Iafrate, Phys. Rev. A **45**, 101 (1992).
[28] Kieron Burke (private communication).
[29] P. Hessler, J. Park, and K. Burke, Phys. Rev. Lett. **82**, 378 (1999).
[30] P. Hessler, N. T. Maitra, and K. Burke, J. Chem. Phys. **117**, 72 (2002).